

# Ph 77 ADVANCED PHYSICS LABORATORY

## – ATOMIC AND OPTICAL PHYSICS –

### Expt. 71 – Fabry-Perot Cavities and FM Spectroscopy

---

---

#### I. BACKGROUND

Fabry-Perot cavities (also called Fabry-Perot etalons) are ubiquitous elements in optical physics, and they are used for such applications as sensitive wavelength discriminators, as stable frequency references, and for building up large field intensities with low input powers. Also, lasers are all made from optical cavities. For our diode lasers, the cavity is made from a semiconductor material a few millimeters in length, and the light propagates inside the semiconductor. Cavities are often made from two curved mirrors as shown in Figure 1.

In this lab you will investigate some cavity properties, and you will see how a cavity can be used as an “optical spectrum analyzer” to measure the spectral content of a laser. In this capacity, you will use the cavity to observe radio-frequency (RF) sidebands on the laser output.

A basic Fabry-Perot cavity consists of two reflectors separated by a fixed distance  $L$ , as is shown in Figure 1; curved reflectors are typically used because such a configuration can trap light in a stable mode. (Two flat mirrors can also make a cavity of sorts, but it is not stable; the light “walks off” perpendicular to the cavity axis.) An excellent detailed discussion of the properties of Fabry-Perot cavities is given by Yariv (1991), and you may want to look through Chapter 4 of this text to better understand the details of cavity physics. Another useful, although somewhat dated, reference is attached as an appendix at the end of this hand-out.

Much of the physics of optical cavities can be understood by considering the flat-mirror case, which reduces the problem to 1D. Physically, this case can be realized if the flat mirrors have effectively infinite extent and the input light can be approximated by a perfect plane wave. For two identical mirrors, each with reflectivity  $R$  and transmission  $T$  ( $R + T = 1$ ), the amplitude of the transmitted and reflected electric field amplitudes (which you will calculate as a prelab problem) are given by

$$\begin{aligned} E_t &= \frac{T e^{i\delta}}{1 - R e^{2i\delta}} E_i \\ E_r &= \frac{(1 - e^{i2\delta}) \sqrt{R}}{1 - R e^{i2\delta}} E_i \end{aligned}$$

where  $E_i$  is the amplitude of the incident light and  $\delta = 2\pi L/\lambda$  is the phase shift of the light after propagating through the cavity (we assume the index of refraction is unity inside the cavity). The transmitted light intensity is then

$$\frac{I}{I_0} = \left| \frac{E_t}{E_i} \right|^2 = \left| \frac{T e^{i\delta}}{1 - R e^{2i\delta}} \right|^2$$

The cavity transmission peaks when  $e^{2i\delta} = 1$ , or equivalently at frequencies  $\nu_m = mc/2L$ , where  $m$  is an integer,  $c$  is the speed of light. At these frequencies the cavity length is an integer number of half-

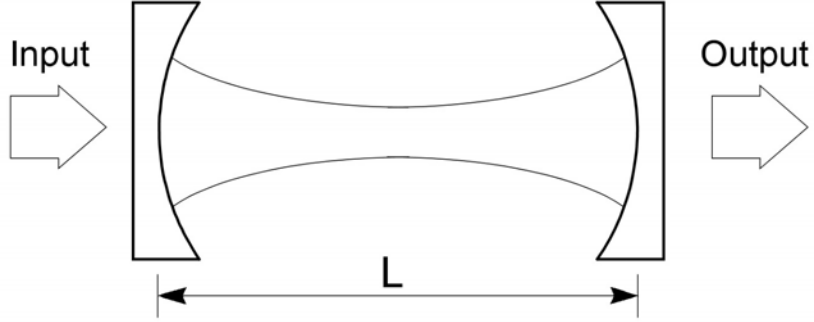


Figure 1. The basic Fabry-Perot cavity. The curved surfaces of the mirrors are coated for high reflectivity, while the flat surfaces are anti-reflection coated and have negligible reflectivity. The curved lines inside the cavity represent the shape of the resonance optical mode.

wavelengths of light. Note that the peak transmission is  $I/I_0 = 1$ , regardless of  $R$ .

The separation between adjacent peaks, called the *free-spectral range*, is given by

$$\begin{aligned}\Delta\nu_{FSR} &= \nu_{m+1} - \nu_m \\ &= \frac{c}{2L}.\end{aligned}$$

If the mirror reflectivity is high (for our cavity mirrors it is approximately 99.5 percent) then the transmission peaks will be narrow compared with  $\Delta\nu_{FSR}$ . The full-width-at-half-maximum,  $\Delta\nu_{fwhm}$ , (*i. e.* the separation between two frequencies where the transmission is half the peak value) is written as

$$\Delta\nu_{fwhm} = \Delta\nu_{FSR}/F,$$

where  $F$  is called the cavity “finesse.” If  $T \ll 1$  the finesse can be shown from the above to be approximately

$$\begin{aligned}F &\approx \frac{\pi\sqrt{R}}{1-R} \\ &\approx \frac{\pi}{T}\end{aligned}$$

The results so far describe an ideal cavity, in which there is no absorption or other loss of light inside the cavity. The peak transmission of such an ideal Fabry-Perot cavity is unity, as can be seen above. Introducing small losses in the cavity leads to the expression

$$E_t = \frac{T\alpha e^{i\delta}}{1 - R\alpha^2 e^{2i\delta}} E_i$$

where  $\alpha$  is a loss parameter (the fractional intensity loss from a single pass through the cavity is equal to  $\varepsilon = 1 - \alpha^2$ ). This gives a peak cavity transmission

$$\frac{I_{peak}}{I_0} \approx \frac{T^2(1 - \varepsilon)}{(T + \varepsilon)^2} \approx \frac{T^2}{(T + \varepsilon)^2}$$

and a finesse

$$F \approx \frac{\pi\alpha\sqrt{R}}{1 - \alpha^2 R}$$

$$\approx \frac{\pi}{T + \varepsilon}$$

It is sometimes useful to think of the Fabry-Perot cavity as an interferometer, and it is also useful to think of it as an optical resonator. If the input laser frequency is not near  $\nu_m$ , the beam effectively just reflects off the first mirror surface (which after all does have a high reflectivity). If the input is equal to  $\nu_m$ , however, then light leaking out from inside the cavity destructively interferes with the reflected beam. Right after turning on the input beam, the power inside the cavity builds up until the light leaking out in the backward direction exactly cancels the reflected input beam, and the beam leaking out in the forward direction just equals the input beam (neglecting cavity losses). Thus at  $\nu_m$  the total cavity transmission is unity, and the light bouncing back and forth in the cavity is  $\sim 1/T$  times as intense as the input beam.

**Problem 1.** Derive the above expressions for  $E_r$  and  $E_t$  as a function of  $\delta$  when  $\varepsilon = 0$ . [Hint: write down a series expression that describes the sums of all the transmitted and reflected beams. Use reflected and transmitted amplitudes  $r$  and  $t$ , where  $r^2 = R$  and  $t^2 = T$ . Then sum the series. Use the fact that if the reflected amplitude is  $r$  for light entering the cavity, then it is  $r' = -r$  for light reflecting from inside the cavity (why? in one case, light is going from in air into glass; in the other case, light is going from glass into air).] Also derive the peak cavity transmission  $I_{peak}/I_0$ , and finesse  $F$ , in the limit  $T, \varepsilon \ll R$ . Plot the transmitted and reflected intensities,  $I_{tran}/I_0$  and  $I_{reflect}/I_0$ , of a cavity as a function of  $\delta$  for  $R = 0.9, 0.95, 0.99$  and  $\varepsilon = 0$ .

**The Optical Spectrum Analyzer.** If we can scan the cavity length, for example by attaching one mirror to a piezo-electric transducer (PZT) tube, as shown in Figure 2, then we can make an interesting gadget called an optical spectrum analyzer. Scanning the spacing  $L$  (which equivalently scans the phase  $\delta$  you used in your calculations) then scans the cavity resonant frequencies  $\nu_m$ . If the laser beam contains frequencies in a range around some  $\nu_0$ , then by scanning the PZT one can record the laser spectrum, as is shown in Figure 2. Note that there is some ambiguity in the spectrum; a single laser frequency  $\nu_0$  produces peaks in the spectrum analyzer output at  $\nu_0 + j\Delta\nu_{FSR}$ , where  $j$  is any integer. If a laser contains two closely spaced modes, as in the example shown in Figure 2, then the output signal is obvious. But if the laser modes are separated by more than  $\Delta\nu_{FSR}$ , then the output may be difficult to interpret.

In the lab, you will scan the laser frequency while keeping the cavity length fixed, but the resulting measurements are basically the same as if you scanned the cavity length.

**Laguerre-Gaussian Modes.** The above analysis strictly holds only for the 1D plane-wave case, and real cavities must have mirrors of finite extent. In this case, it's best to think of Fabry-Perot cavities as full 3D optical resonators, rather than simply a set of two mirrors. By curving the mirrors, the cavity supports a set of trapped normal modes of the electromagnetic field, known as *Laguerre-Gaussian modes*. As long as the cavity has cylindrical symmetry, the transverse mode patterns are described by a combination of a

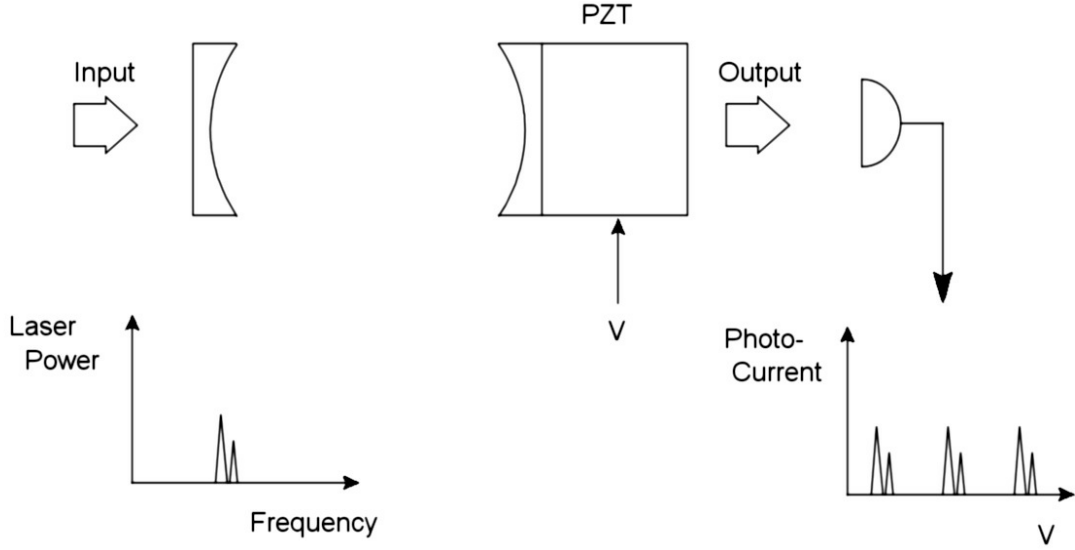


Figure 2. Using a Fabry-Perot cavity as an optical spectrum analyzer. Here the input laser power as a function of frequency  $P(f)$  is shown with a multi-mode structure. By scanning the cavity length with a piezoelectric (PZT) tube, the laser's mode structure can be seen in the photodiode output as a function of PZT voltage  $I(V)$ . Note the signal repeats with the period of the cavity free-spectral range.

Gaussian beam profile with a Laguerre polynomial. The modes are labeled by  $TEM_{p\ell}$ , where  $p$  and  $\ell$  are integers labeling the radial and angular mode orders. The intensity at a point  $r, \phi$  (in polar coordinates) is given by

$$I_{p\ell}(r, \phi) = I_0 \rho^\ell [L_p^\ell(\rho)]^2 \cos^2(\ell\phi) e^{-\rho}$$

where  $\rho = 2r^2/w^2$  and  $L_p^\ell$  is the associate Laguerre polynomial of order  $p$  and index  $\ell$ . The radial scale of the mode is given by  $w$ , and modes preserve their general shape during propagation. A sample of some Laguerre-Gaussian modes is shown in Figure 3.

This figure displays the transverse mode profiles; the longitudinal profile of the mode is that of a standing wave inside the cavity, which has some number  $n$  of nodes. The various modes with different  $n, p$ , and  $\ell$  in general all have different resonant frequencies. The  $TEM_{00}$  mode has a simple Gaussian beam profile, and this is the mode one usually wants to excite inside the cavity. Lasers typically use this mode, and thus generate Gaussian output beams. As you will see in the lab, however, it is not always trivial to excite just the  $TEM_{00}$  mode inside a cavity.

Note that the mode shape shown in Figure 1 essentially shows  $w$  for a  $TEM_{00}$  mode as a function of position inside the cavity. The mode has a narrow *waist* at the center of the cavity, and diffraction causes the beam to expand away from the center. At the waist, the wavefronts of the electric field (or equivalently the nodes of the standing wave) are flat and perpendicular to the cavity axis. At the mirrors, the wavefronts are curved and coincide with the mirror surfaces, so the wave reflects back upon itself.

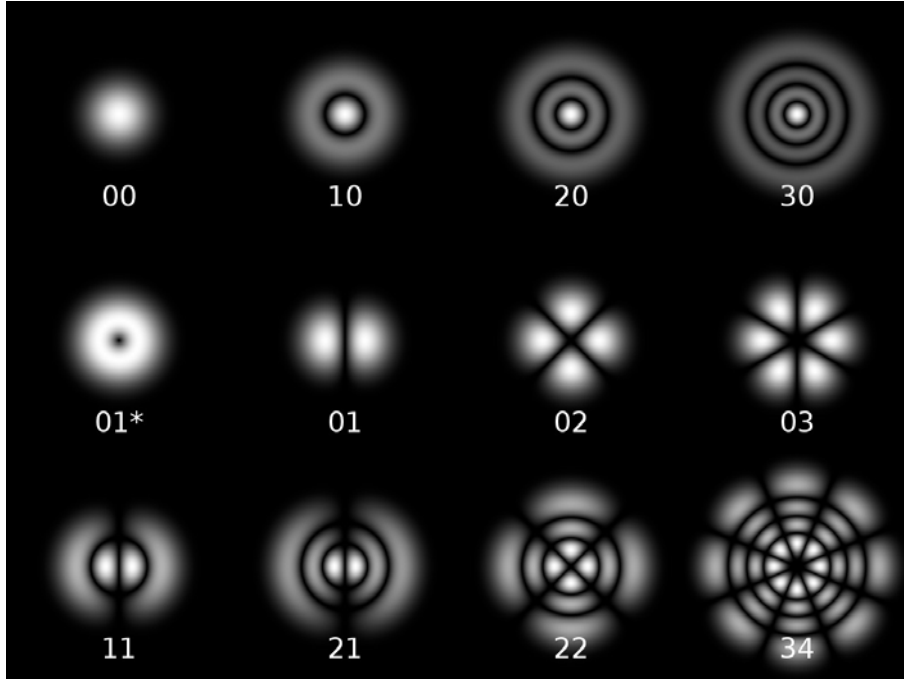


Figure 3. Several Laguerre-Gaussian modes, which are the electromagnetic normal modes inside a Fabry-Perot cavity. The  $\text{TEM}_{01}^*$  mode, called a doughnut mode, is a superposition of two (degenerate)  $\text{TEM}_{01}$  modes rotated  $90^\circ$  with respect to one another.

**Confocal Resonators.** An interesting (and useful) degeneracy occurs if we choose the cavity length to be equal to the radius of curvature of the Fabry-Perot mirrors,  $L = R_{\text{mirror}}$ . In this case, the mode frequencies of the various transverse modes all become degenerate with a separation of  $c/4L = \Delta\nu_{FSR}/2$  (see Yariv, Section 4.6, for a derivation of this). For this special case, called a “confocal” cavity, the spectrum will look just like that shown in Figure 2, except the mode spacing will be  $\Delta\nu_{\text{confocal}} = c/4L$ . The width of the transmission peaks  $\Delta\nu_{\text{fwhm}}$  stays roughly the same in principle, but in practice  $\Delta\nu_{\text{fwhm}}$  depends on how well the cavity is aligned, and how precisely we have  $L = R_{\text{mirror}}$ .

Another nice feature of the confocal cavity is that the cavity transmission is insensitive to laser alignment. Figure 4 shows that each resonant mode in the confocal cavity can be thought of as a “bow-tie” mode, which traverses the cavity twice before retracing its path – hence  $\Delta\nu_{\text{confocal}} = c/4L$ . This is a crude picture, but it can be helpful in understanding the confocal cavity. It shows you in a rough way how the output spectrum might be insensitive to alignment, since the bow-tie modes are excited no matter where the beam enters the cavity. You will work with a confocal and non-confocal cavity in the lab, and hopefully this will all make good sense once you see it all in action.

**FM Spectroscopy.** In the radio-frequency domain, there exists a substantial technology built up around amplitude-modulation and frequency-modulation of an electromagnetic carrier wave (which gives us, for example, AM and FM radio broadcasting). If one boosts the typical carrier wave frequency from 100 MHz

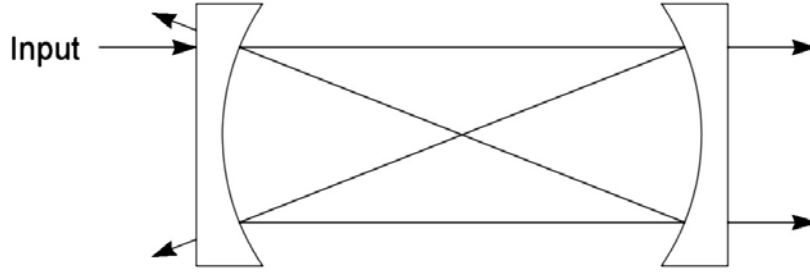


Figure 4. Ray paths for a confocal Fabry-Perot cavity (the off-axis scale is exaggerated).

(FM radio) to 500 THz (optical), the same ideas apply to AM and FM modulation of lasers. The resulting optical technology has many applications, the most dominant one being fiber-optic communications.

Modulating the injection current to the diode laser is a very simple way to modulate the laser output, both in frequency and amplitude. (Using non-linear crystal modulators is another way to modulate a laser beam.) The basic idea is that one drives the laser with an injection current which consists of a large DC part and a small high-frequency AC part on top. The AC part produces both AM and FM modulation of the laser, but we will ignore the smaller AM part for now.

For pure frequency modulation, we can write the electric field of the laser beam at some fixed location as:

$$\vec{E}(t) = \vec{E}_0 \exp(-i\omega_0 t - i\phi(t))$$

where  $\phi(t)$  is the modulated phase of the laser output. We always assume that  $\phi(t)$  is slowly varying compared to the unmodulated phase change  $\omega_0 t$ , since  $\omega_0$  is at optical frequencies, and our modulation will be at radio frequencies. If we're putting in a single sinusoidal phase modulation we have

$$\phi(t) = \beta \sin(\Omega t)$$

where  $\Omega$  is the modulation frequency, and  $\beta$ , called the modulation index, gives the peak phase excursion induced by the modulation. If we note that the instantaneous optical frequency is given by the instantaneous rate-of-change of the total phase, we have

$$\begin{aligned} \omega_{\text{instant}} &= \omega_0 + d\phi/dt \\ &= \omega_0 + \beta\Omega \cos(\Omega t) \\ &= \omega_0 + \Delta\omega \cos(\Omega t) \end{aligned}$$

where  $\Delta\omega$  is the maximum frequency excursion. Note that  $\beta = \Delta\omega/\Omega$  is the dimensionless ratio of the maximum frequency excursion to frequency modulation rate.

It is useful to expand the above expression for the electric field into a carrier wave and a series of

sidebands

$$\begin{aligned}
 \vec{E}(t) &= \vec{E}_0 \exp[-i\omega_0 t - i\beta \sin(\Omega t)] \\
 &= \vec{E}_0 \sum_{n=-\infty}^{n=\infty} J_n(\beta) \exp[-i(\omega_0 + n\Omega)t] \\
 &= \vec{E}_0 \left\{ J_0(\beta) \exp(-i\omega_0 t) + \sum_{n=1}^{n=\infty} J_n(\beta) [\exp[-i(\omega_0 + n\Omega)t] + (-1)^n \exp[-i(\omega_0 - n\Omega)t]] \right\}
 \end{aligned}$$

This transformation shows that our original optical sine-wave has now developed a comb-like structure in frequency space. The  $J_0$  term at the original frequency  $\omega_0$  is the optical “carrier” frequency (in analogy with radio terminology), while the other terms at frequencies  $\omega_0 \pm n\Omega$  form sidebands around the carrier. The sideband amplitudes are given by  $J_n(\beta)$ , which rapidly becomes small for  $n > \beta$ . Note that the total power in the beam is given by

$$\bar{E} \cdot \bar{E}^* = E_0^2 \left[ J_0^2(\beta) + 2 \sum_{n=1}^{n=\infty} J_n(\beta)^2 \right] = E_0^2$$

which is independent of  $\beta$ , as it must be for pure frequency modulation. Often one wishes to add two small sidebands around the carrier, for which one wants  $\beta \ll 1$ , and the sideband power is then given by  $\sim J_1(\beta)^2 \approx \beta^2/4$ . Evaluating the above sum, and convolving with a Lorentzian laser+cavity spectrum gives an output power

$$I(\omega) = J_0^2(\beta)L(\omega; \omega_0) + \sum_{n=1}^{n=\infty} J_n(\beta)^2 [L(\omega; \omega_0 + n\Omega) + L(\omega; \omega_0 - n\Omega)]$$

where  $L(\omega; \omega_0)$  is a normalized Lorentzian function centered at  $\omega_0$ .

**Problem 2.** Evaluate and plot the above optical spectrum, as you might expect to see it using your Fabry-Perot optical spectrum analyzer (remember that a photodiode measures optical *power*, not electric field amplitude). Plot versus frequency  $\nu = \omega/2\pi$ , which is what a frequency meter reads. Assume a Lorentzian laser+cavity linewidth of  $\Delta\nu = 10$  MHz. Plot three curve with: 1)  $\Omega/2\pi = 120$  MHz,  $\beta = 0.5$ ; 2)  $\Omega/2\pi = 30$  MHz,  $\beta = 1.5$ ; and 3)  $\Omega/2\pi = 1$  MHz,  $\beta = 20$ . Note for the last plot you will have to evaluate the sum up to fairly high  $n$ , at least to  $n > \beta$ . For  $\beta \gg 1$ , note that the spectrum looks much like what you would expect for slowly scanning the laser frequency from  $\omega_0 - \beta\Omega$  to  $\omega_0 + \beta\Omega$ .

## II. LABORATORY EXERCISES.

Your first task in this lab is to look at the light transmitted through a simple cavity using the set-up shown in Figure 5. Use the ramp generator in the laser controller to scan the laser frequency (ask your TA how), and monitor the photodiode output on the oscilloscope.

In order to get any light through the cavity, you need to align the incoming laser beam so that: 1) the beam hits the center of the first mirror, and 2) the beam is pointed down the cavity axis. The mirrors M1 and M2 provide the necessary adjustments to align the incident beam, and note that the different degrees of freedom are nicely decoupled – M1 mostly changes the laser position at the cavity, and M2 mostly changes the angle of the entering beam.

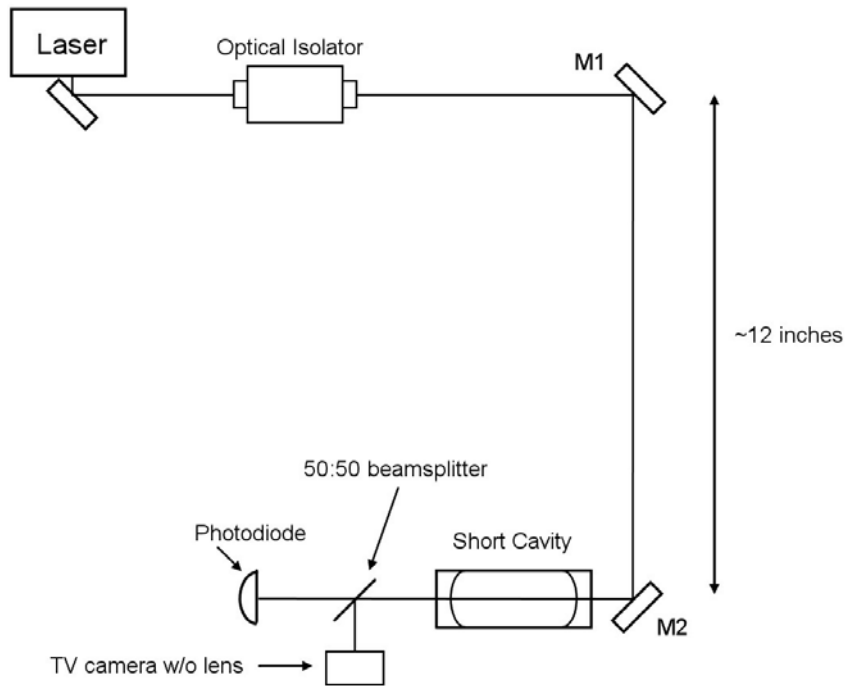


Figure 5. Optics set-up to view the light transmitted through the short cavity.

First adjust M1 so the beam is centered on the cavity, and then adjust M2 so the backreflected beam coincides with the incident beam. Use a white card with a hole in it to see the position of the backreflected beam. Iterate as necessary.

When this looks good, place a white card behind the cavity to view the transmitted beam. It will be faint, but you should be able to see a pair of bright spots, or perhaps a bright ring, on the card. To bring the transmitted beam to a single spot, you will probably need to “walk” the input beam, which is a way to systematically sample the 4-dimensional alignment space defined by the four adjustments of M1 and M2. Your TA can show you how. Once you have the transmitted beam down to a single, sharp spot, place the photodiode to intercept the beam, and place the TV camera to view the shape of the beam.

With the sweep on, you should see a forest of peaks on the transmitted signal. Each peak corresponds to a single cavity mode you are exciting with the laser. Each  $TEM_{npl}$  mode has a slightly different frequency, so each gives a separate peak. In addition, the spectrum repeats with a period of  $\Delta\nu_{FSR}$ . If you tweak the alignment of the incoming beam slightly, you will see the peaks all change height. This is because you excite different modes with different alignments.

With the sweep off, you can examine the shapes of the different modes using the TV camera. Move the piezo DC offset adjust to select different modes. Compare with Figure 3 above. **Print out an oscilloscope trace showing a typical scan, and tape it into your notebook.**

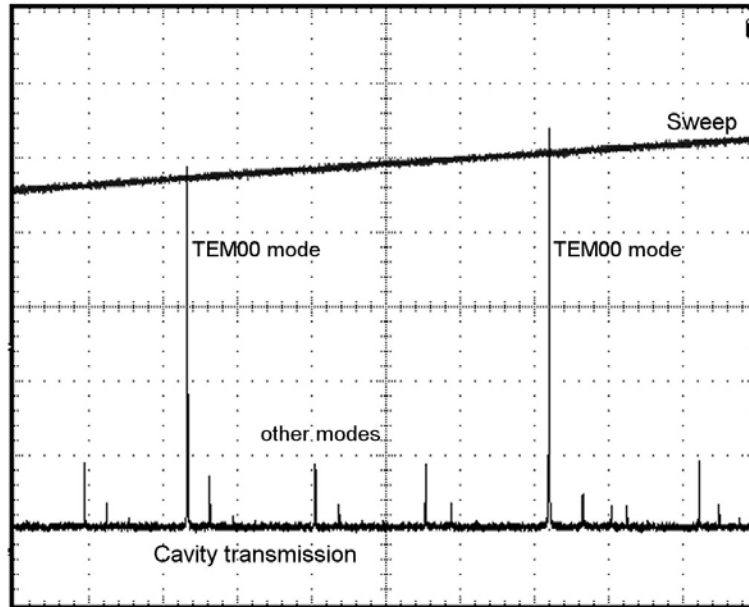


Figure 6. The cavity transmission with fairly good mode matching. Note the dominant  $TEM_{00}$  modes separated by  $\Delta\nu_{FSR}$ . The peaks heights are very sensitive to alignment and even to vibration.

**Mode Matching.** Now you should try to excite just the  $TEM_{00}$  mode of the cavity, which means you have to *mode match* the incoming beam to the cavity mode. If you think about the mode inside the cavity (see Figure 1), you can see that the beams leaking out of the cavity diverge in both directions. You can see this if you use a white card with a hole in it placed far from the cavity. The reflected beam from the cavity will make a large spot on the card, much larger than the incoming beam. Thus the input beam is not well matched to the cavity modes.

To match the  $TEM_{00}$  mode, the incoming beam should be converging. You can achieve this by placing a 500mm focal length lens about 11 inches in front of the cavity. Before aligning the cavity, note that the size of the reflected beam is now about equal to the incoming laser size, so the mode match is better than before.

Align the cavity with the lens in place and view the transmitted signal. You should see fewer large modes. Turn the sweep down to identify the different modes on the TV. Find the  $TEM_{00}$  mode, and tweak the mirror alignment to maximize this mode while minimizing the others. With some effort, you can produce a transmitted signal that looks something like that shown in Figure 6, with dominant  $TEM_{00}$  peaks separated by  $\Delta\nu_{FSR}$ . You cannot do much better than this, even in theory, for two reasons: 1) the mode-matching lens is actually not quite right to match to the cavity, so you are bound to excite some other modes; and 2) the incoming laser beam is itself not a perfect  $TEM_{00}$  mode (expand the beam with a lens and you can see that it doesn't have a perfect Gaussian shape), which means it contains other modes

at some level. **Print out a trace showing your best TEM<sub>00</sub> modes.**

**The Confocal Cavity.** The next task is to set up the confocal Fabry-Perot cavity as shown in Figure 7 and to look at some of its properties. Unlike the previous cavity, the confocal cavity is insensitive to the precise alignment and mode matching of the input beam, because the different transverse modes are degenerate in frequency (see the discussion in Section I above). Nevertheless, you still have to align things reasonably well, using the same procedures described above.

**Observe the Mode Structure of the Cavity.** Align the input beam and adjust the cavity length until the transmitted signal shows a series of sharp peaks (much different than with the non-confocal cavity!). Tweak the cavity length so the peaks are narrow and symmetrical, which should maximize the transmitted peak intensity. Once that looks good, change the cavity length by a large amount (say 10 turns of the mounting tube) and observed the transmitted spectrum. As the cavity length is changed away from the confocal length, the transverse modes are no longer degenerate. At first, you see the peaks broaden and become asymmetrical. Then, as you change the length more, you can see individual mode peaks show up. Change the input beam alignment to see the different modes change in amplitude. **Print out a few spectra with different cavity lengths.**

**Measure the Transmitted and Reflected Intensities.** Adjust the cavity length to its confocal value, and align the input beam to maximize the height of the transmitted peaks. Tweak the length and alignment with some care to produce sharp, symmetrical peaks with the highest possible amplitude. When that looks good, insert a "pick-off" mirror somewhere in the beam and send it to the second photodiode. Use the mirror to maximize the photodiode signal on the oscilloscope (so the beam is centered on the photodetector), and measure the output voltage (and note the photodiode gain). It works well to use the "measure" feature on the oscilloscope to measure the average output voltage. With care, you could convert this voltage to milliwatts of laser power, but you will be taking power ratios, so you don't need this conversion.

Without changing the cavity alignment, set up the second lens and photodiode as shown in Figure 7. Again make sure the beam is centered on the photodetector and measure the output signal. The value should be about 25% of what you measured previously (because the beam intensity was diminished twice by the 50:50 beamsplitter). If you don't get within a few percent of that value, something is wrong (probably the alignment).

Next send the first photodiode signal directly into the oscilloscope along with the second. Note that the dips in reflected light correspond to the peaks in transmitted light, as you would expect. Measure the peak widths and make sure they are greater than 20  $\mu$ sec, so that the photodiode is fast enough to record the full peak. If not, use a slower scan. **Measure the height of the transmitted peaks and compare with the input beam intensity, to produce a peak transmitted fraction.** Keep in mind the photodiode gains, which may be different, and how many times the various beams went through the beamsplitter. You should be able to produce a transmitted fraction between 5% and 10%. If your measurement is above 10%, you probably made an error somewhere (or your cavity alignment is amazingly good). If

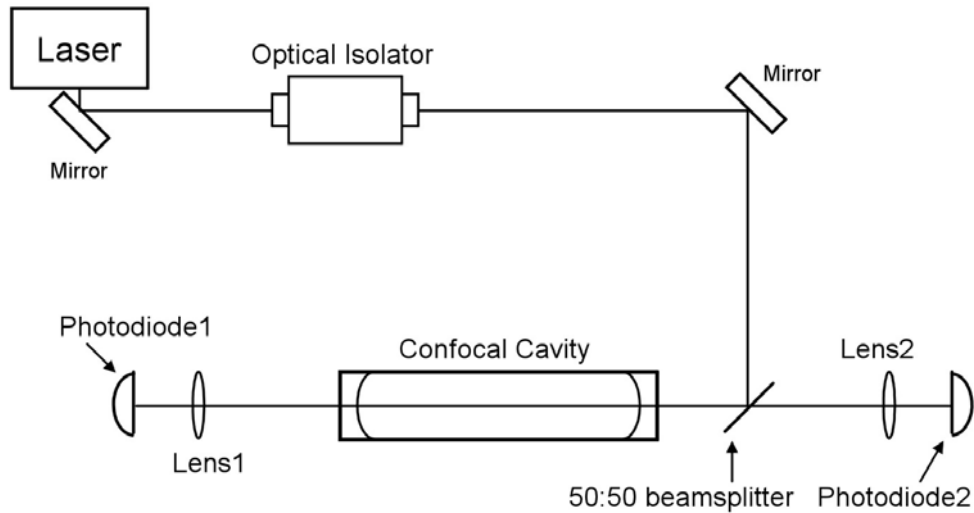


Figure 7. Optics set-up for the confocal cavity.

your measurement gives you something below 5%, again check for simple errors. If that's not it, tweak the cavity length and alignment until the peak transmitted fraction is above 5%. When everything looks good, **print out the spectrum showing sharp peaks.**

**Measure the Cavity Finesse.** Capture a single sweep on the oscilloscope and use the built-in cursors to measure the effective finesse of the cavity. Measure the spacing between the peaks (the free spectral range) and then change the time-base on the 'scope and measure the full-width at half-maximum of the peaks. The effective finesse is then  $F = \Delta\nu_{FSR}/\Delta\nu_{FWHM}$ . You should get  $F > 100$  or even  $F > 200$  if the cavity is well aligned.

Why is the transmitted peak intensity only 5%, when in principle it could be 100%? Part of the reason is losses inside the cavity, as described in the discussion in Section I, but that's only a small part. Calculate about how great the losses would have to be to produce a 5% transmitted intensity, assuming a mirror transmission of 1%. The actual mirror losses are probably less than 0.1% per bounce (unless the mirrors are very dirty, which they shouldn't be).

The main reason for the low transmitted intensity is that the mode degeneracy is not perfect. If you change the cavity length or input beam alignment only slightly, you can see the peak height drop quickly. Since the input beam is not mode-matched to the cavity, the transmitted intensity of any given mode is fairly low. And if the modes are not perfectly degenerate, they don't overlap well, resulting in a low peak intensity. With a non-confocal cavity and a well mode-matched beam, it is possible to achieve a peak transmitted intensity close to 100%. However, for simply looking at the frequency structure of a laser (i.e., with an optical spectrum analyzer), the confocal cavity is quite convenient to use, even with its lower transmitted intensity.

**FM Spectroscopy.** Next you should observe the FM spectra you calculated in the prelab exercises, using the confocal Fabry-Perot cavity as an optical spectrum analyzer. With the transmitted signal showing nice sharp peaks, reduce the sweep to zoom in on a single peak. Then take the RF function generator, turn it on, and feed it into the RF Input BNC of the diode laser. (NOTE: Do not disconnect the cable from its connection at the laser. The laser is sensitive to static discharge, which can easily burn out the diode. Also turn the RF generator on *first*, and then feed the output into the laser. This helps avoid voltage spikes that may occur when you turn the generator on.)

As you vary the oscillator frequency  $\Omega/2\pi$  and the amplitude (which changes  $\Delta\omega$  and thus  $\beta$ ), you should observe the range of behavior you calculated. **Record several traces that correspond as closely as you can achieve to your three calculated plots.** You should get pretty good agreement (if not, check with the TA). One significant difference between calculated and measured spectra is that the measured spectra may be asymmetric. This is due to residual *amplitude* modulation of the laser, which we did not include in our pure FM calculation.

**Measure the Free-Spectral Range.** Finally, put two high-frequency sidebands on your laser, **print out a spectrum**, and use the known sideband frequency to measure the free-spectral-range of the Fabry-Perot cavity. Compare with what you expect for a cavity length of 20 cm (equal to the radius of curvature of the mirrors).

### III. REFERENCES

Yariv, A. 1991, *Optical Electronics*, Saunders College Publishing, 4th ed.

# Spectra-Physics Laser Technical Bulletin Number 6



PUBLISHED BY SPECTRA-PHYSICS, INCORPORATED • MOUNTAIN VIEW • CALIFORNIA

## Scanning Spherical-Mirror Interferometers For The Analysis of Laser Mode Structure

### I. Introduction

Scanning spherical-mirror interferometers<sup>1</sup> have become common tools for the analysis of laser radiation. They are very high-resolution spectrometers, and can be used to provide information concerning laser mode structure that is difficult to obtain using any other instrument.

For a variety of practical reasons, scanning spherical-mirror interferometers have been difficult to use. Recently, however, it has been found that certain special types of these interferometers are comparatively easy to use: these special types of interferometers are "mode-degenerate" interferometers. Of the mode-degenerate interferometers, the most useful is the confocal interferometer, first described, in a somewhat different form than is now common, by Connes<sup>2</sup>.

The principal reason for the interest in using scanning spherical-mirror interferometers to study laser radiation is, of course, that the light emitted by most ordinary gas lasers is not perfectly monochromatic. The beam from a typical gas laser contains several discrete optical frequencies, separated from each other by frequency differences of "radio-frequency" magnitude ( $10^8 - 10^9$  Hz). These different optical frequencies can be associated with different modes of oscillation of the laser.

It is common practice to distinguish two types of laser modes: "longitudinal" modes differ from one another only in their oscillation frequency; "transverse" modes differ from one another not only in their oscillation frequency, but also in their field distribution in a plane perpendicular to the direction of propagation. Corresponding to a given transverse mode are a number of longitudinal modes which have the same field distributions as the given transverse mode but differ in frequency; it is not customary, however, to associate different transverse modes with a given longitudinal mode.

Most applications of gas lasers require that the laser operate in a single transverse mode. Moreover, in most cases, the laser must operate in the lowest order ( $TEM_{00}$ ) transverse mode. The reason for this concerns the amount of power that can be focused in a diffraction-limited beam: more power can be focused in such a beam when the laser operates in the lowest-order transverse mode than when it operates in high-order transverse modes<sup>3</sup>.

In many applications of gas lasers, the longitudinal mode structure of the laser beam is also important. In holography, for example, the presence of several longitudinal modes limits the coherence length of the emitted light, and hence the depth of field of holograms made with it. In many communications experiments, the presence of several longitudinal modes may give rise to distortion effects. In some spectroscopic applications, the resolution is limited by the number of oscillating longitudinal modes.

As mentioned above, the scanning spherical-mirror interferometer is a powerful tool for studying the mode structure of gas lasers. There are, however, other methods which are used to study laser mode structure. The most common of these employs a radio-frequency spectrum analyzer. When a laser beam is detected by a photodetector, the output current from the photodetector will contain signals at the difference frequencies between the various modes of the laser beam. By measuring the frequencies and amplitudes of the various difference-frequency signals, some characteristics of the optical spectra can be deduced.

Radio-frequency measurements have some advantages and some disadvantages over direct optical-frequency measurements, such as those obtained from scanning spherical-mirror interferometers. Radio-frequency measurements usually have higher resolution than optical-frequency measurements.

On the other hand, conventional radio-frequency measurements do not give complete information about the optical mode spectra.

Consider the case of a laser beam containing two modes, one large in amplitude, and one small in amplitude. If such a beam is detected by a photodetector, the output current will contain a signal which oscillates at a frequency equal to the difference frequency between the two modes. However, there will be no way to determine whether the strong mode is the higher-frequency mode or the lower-frequency mode. Both situations will give the same radio-frequency output signal. With direct optical-frequency spectroscopy, this ambiguity does not occur: the output signal gives complete information regarding the spectrum.

Radio-frequency measurements are most useful when it is only necessary to detect the presence or absence of certain modes in a laser beam. In general, direct optical-frequency measurements are easier to interpret and easier to perform.

## II. The Fabry-Perot Interferometer

Scanning spherical-mirror interferometers belong to the general class of multiple-beam interferometers. The most common multiple-beam interferometer is the Fabry-Perot etalon, which consists of two plane mirrors which are placed parallel to one another, separated by a distance  $d$ . The resonance condition for such an interferometer is that the spacing between the mirrors be equal to an integral number of half wavelengths of the incident light. If the interferometer is illuminated at normal incidence with a collimated beam of frequency  $\nu_0$ , the resonance condition is

$$\nu_0 = \frac{mc}{2d}, \quad (1)$$

where  $m$  is an integer and  $c$  is the velocity of light.

More generally, it can be shown that the transmittance of the etalon is given by the famous Airy formula

$$\frac{I}{I_0} = \frac{1}{\left(1 + \frac{A}{T}\right)^2} \frac{1}{1 + \frac{4R}{(1-R)^2} \sin^2 \frac{2\pi\nu d}{c}}, \quad (2)$$

where  $I_0$  is the intensity of the beam incident on the interferometer,  $I$  is the intensity of the beam emerging from the interferometer,  $R$  is the reflectance of the mirrors,  $T$  is the transmittance of the mirrors, and  $A$  is the "dissipative" loss of the mirrors.

For high-reflectance mirrors (typical of modern Fabry-Perot etalons) the transmission "fringes" are extremely sharp. Under these conditions, the transmittance of the Fabry-Perot etalon will be

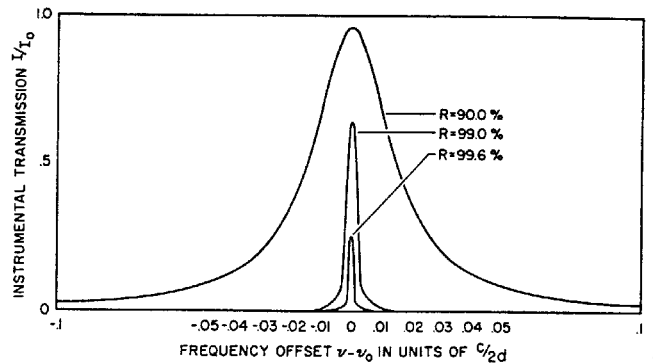
negligible unless the sine term is nearly zero. We may thus use the approximations  $\sin \theta \approx \theta$  and  $R \approx 1$  to write the Airy formula as

$$\frac{I}{I_0} = \frac{1}{\left(1 + \frac{A}{T}\right)^2} \frac{1}{1 + \left(\frac{4\pi d}{c(1-R)}\right)^2 (\nu - \nu_0)^2}. \quad (3)$$

This formula is illustrated graphically in Figure 1. We see that near a transmission fringe, the transmittance of a Fabry-Perot etalon is a Lorentzian function of frequency having a full-width at half maximum of

$$\Delta\nu = \frac{c(1-R)}{2\pi d}. \quad (4)$$

The quantity  $\Delta\nu$  is called the "instrumental bandwidth" of the etalon.



1. Transmittance of a Fabry-Perot etalon for various mirror reflectances. The "dissipative" loss of the mirrors is assumed to be 0.2%.

Note from (1) that the difference in frequency between two transmission fringes, called the "free-spectral-range" of the etalon, is given by

$$\text{FSR} = \frac{c}{2d}. \quad (5)$$

The ratio of the free-spectral-range to the instrumental bandwidth is called the "finesse" of the etalon. Using (4) and (5), we find for the finesse

$$F = \frac{\pi}{(1-R)}. \quad (6)$$

The ratio of the transmission frequency to the instrumental bandwidth is known as the resolving power, or "Q" (quality factor) of the etalon. We thus have

$$Q = \frac{2\pi\nu d}{c(1-R)}. \quad (7)$$

The Fabry-Perot etalon, although it is a versatile tool for the high-resolution spectroscopy of ordinary light sources, is of limited usefulness in analyzing laser mode structure. The reason for this is that an ordinary Fabry-Perot etalon does not have

sufficient resolving power to be very useful in analyzing laser beams.

A typical gas-laser transition has a Doppler linewidth of a few gigahertz. The various modes of the laser are typically separated by a few tens of megahertz. In order for an interferometer to be useful in analyzing laser mode spectra, it should have a free-spectral-range which is larger than the Doppler linewidth and an instrumental bandwidth which is small compared to the frequency differences between the various modes of the laser; in short, it should have a high finesse. For analyzing laser mode spectra, it is usually desirable to employ an interferometer having a finesse of at least one hundred.

It is very difficult to make Fabry-Perot etalons which have a finesse of 100. A typical value for the finesse of a Fabry-Perot etalon is  $\approx 30$ , although it is possible to obtain somewhat higher values with high-quality instruments.

Two principal factors limit the finesse of Fabry-Perot etalons. The surface figure of the mirrors must be flat to approximately the transmission wavelength divided by the finesse of the interferometer. Thus, an interferometer having a finesse of 100 must have mirrors which are flat to 1/100 wavelength over the useful aperture. If the aperture of the interferometer is small enough, the mirrors may indeed appear flat to within 1/100 wavelength. However, if the aperture is made small, diffraction effects which limit the finesse of the interferometer become important.

The Airy formula given above neglects the effects of diffraction. If the diameter of the interferometer mirrors is large compared to their separation, diffraction is not important. However, if a small aperture is placed within the interferometer in an attempt to improve the effective figure of the mirrors, diffraction effects at the edges of the aperture cause a "loss" in the interferometer which is equivalent to a reduction in the reflectance of the mirrors. This equivalent reduction in reflectance limits the finesse of the interferometer.

### III. Spherical-Mirror Interferometers

The diffraction effects which are characteristic of Fabry-Perot etalons can, to a large extent, be eliminated by using spherical mirrors in the interferometer. The radii of curvature of the mirrors (which, for the sake of simplicity, we assume to be equal) must be greater than one half their separation.

The diffraction loss of a spherical-mirror interferometer is orders of magnitude lower than that of a Fabry-Perot interferometer, and is usually small enough to be negligible. In addition, the surface figure on the mirrors of a spherical-mirror

interferometer is considerably less critical than the figure on the mirrors of a Fabry-Perot interferometer. The reason for this comparatively large figure tolerance is that only a small area (typically  $< 1 \text{ mm}^2$ ) of the spherical-mirror interferometer mirrors is useful. Thus, mirrors which are good to within 1/10 wavelength over their entire area may contain small areas having a figure of better than 1/100 wavelength.

The salient characteristic of a general spherical-mirror interferometer is that it must be illuminated with a narrow, diffraction-limited beam to work properly. In laser terminology, it must be "mode-matched" to the laser which is to be analyzed.

The various modes of a spherical-mirror cavity resonate at frequencies given by

$$\nu_0 = \frac{c}{2d} \left[ q + \frac{1}{\pi} (1 + m + n) \cos^{-1} \left( 1 - \frac{d}{R} \right) \right], \quad (8)$$

where  $c$  is the velocity of light,  $d$  is the separation of the mirrors,  $R$  is the radius of curvature of the mirrors,  $q$  is an integer denoting the longitudinal-mode number, and  $m$  and  $n$  are integers denoting the transverse-mode numbers.

A spherical-mirror interferometer will have a high transmission for frequencies which satisfy the resonance condition (8). The resonance frequencies corresponding to different values of  $q$  define the different longitudinal modes of the interferometer. The resonance frequencies corresponding to different values of  $m$  and  $n$  define the different transverse modes of the interferometer. Note that to any specific transverse mode there correspond a number of longitudinal modes.

The frequency separation of any two interferometer resonances defines the free-spectral-range of the interferometer. In order for the free-spectral-range of the interferometer to be large enough to be useful, it is necessary to restrict the excitation of the interferometer to a single transverse mode. The various longitudinal modes corresponding to that transverse mode then determine the free-spectral-range to be  $c/2d$ , as is the case for the Fabry-Perot etalon. In practice, the only transverse mode of the interferometer which is convenient to excite is the lowest-order ( $\text{TEM}_{00}$ ) mode.

The requirement that a general spherical-mirror interferometer be excited in a single transverse mode causes considerable complication in practical applications of the device. In order to match the laser beam into the  $\text{TEM}_{00}$  mode of the interferometer, the laser itself must operate in the  $\text{TEM}_{00}$  mode. In addition, the interferometer must be carefully aligned so that its axis corresponds to the propagation axis of the incoming laser beam. When such alignment is accomplished, light reflected

from the interferometer travels back into the laser and perturbs the modes of the laser. It is thus necessary to use an optical isolator between the laser and the interferometer. Finally, the beam diameter and divergence of the incoming laser beam must be matched to the beam diameter and divergence of the TEM<sub>00</sub> mode of the interferometer.

If the above conditions are not fulfilled, the interferometer will not work properly. The most serious defect of general spherical-mirror interferometers is that if they are not properly mode-matched to the incoming laser beam, they will have "spurious" transmission fringes. These fringes are caused by the excitation of high-order transverse modes of the interferometer, which generally resonate at different frequencies than the TEM<sub>00</sub> mode.

The above requirements make the general spherical-mirror interferometer rather difficult to use. Fortunately, by using special forms of spherical-mirror interferometers, these requirements can be considerably relaxed. These special forms of spherical-mirror interferometers are called "mode-degenerate" interferometers.

#### IV. Mode-Degenerate Interferometers

For practical applications, mode-degenerate interferometers are more useful devices than are general spherical-mirror interferometers. The fundamental reason for this is that mode-degenerate interferometers do not need to be mode-matched to the incident laser beam. This fact permits considerable simplification in the experimental use of mode-degenerate interferometers. Specifically:

1. Since the transverse modes of the laser do not need to be matched to the transverse modes of the interferometer, it is not necessary that the laser operate in a single transverse mode.

2. There are no "spurious" resonances in mode-degenerate interferometers.

3. Since mode-matching is not required, the interferometer need not be accurately located on the axis of the incident laser beam; this reduces the required alignment tolerance of the interferometer.

4. When the axis of the interferometer does not coincide with the axis of the incident laser beam, the light reflected by the interferometer does not travel back into the laser and perturb the laser oscillation. It is thus usually desirable to use the interferometer with off-axis illumination.

A mode-degenerate interferometer is a spherical-mirror interferometer whose transverse modes are degenerate in frequency. The operation of such interferometers can be understood by considering that, if the radii of curvature and separation of the mirrors of a spherical-mirror interferometer satisfy the equation

$$\cos^{-1} \left( 1 - \frac{d}{R} \right) = \frac{\pi}{l}, \quad (9)$$

where  $l$  is an integer, then the resonance equation (8) can be written as

$$\nu_0 = \frac{c}{2ld} [lq + 1 + m + n] \quad (10)$$

Since increasing the sum  $(m+n)$  by  $l$  and decreasing  $q$  by one leaves the resonant frequency of the interferometer unchanged, it follows that the interferometer will have  $l$  "sets" of degenerate transverse modes. These  $l$  "sets" of modes will be equally separated in frequency.

The best-known mode-degenerate interferometer is the confocal interferometer, which corresponds to  $l=2$ . The confocal interferometer has "even-symmetric" modes corresponding to  $(m+n)$  even, and "odd-symmetric" modes, corresponding to  $(m+n)$  odd. The even-symmetric mode resonances fall exactly halfway between the odd-symmetric mode resonances. Thus the free-spectral-range of a confocal interferometer, when it is illuminated simultaneously in several transverse modes, is  $c/4d$ , rather than  $c/2d$ .

In general, the free-spectral-range of an  $l$ -fold mode-degenerate interferometer is given by

$$\text{FSR} = \frac{c}{2ld} \quad (11)$$

The transmittance of an  $l$ -fold mode-degenerate interferometer is given by

$$\frac{I}{I_0} = \frac{T^2 \sum_{j=1}^l R^{2(j-1)}}{(1-R^l)^2} \frac{1}{1 + \frac{4R^l}{(1-R^l)^2} \sin^2 \frac{2\pi\nu ld}{c}} \quad (12)$$

Note that, if  $l=1$ , the above equation reduces to the Airy formula (2). If the reflectance of the mirrors is close to unity, we find for the transmittance of the interferometer near a resonant frequency:

$$\frac{I}{I_0} = \frac{1}{l \left( 1 + \frac{A}{T} \right)^2} \frac{1}{1 + \left( \frac{4\pi d}{c(1-R)} \right)^2 (\nu - \nu_0)^2} \quad (13)$$

The instrumental bandwidth is thus given by

$$\Delta\nu = \frac{c(1-R)}{2\pi d}; \quad (14)$$

the resolving power by

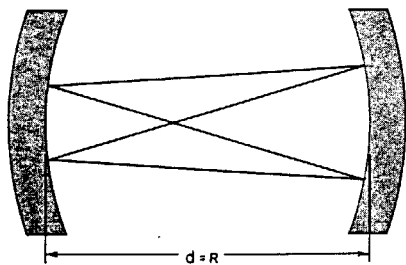
$$Q = \frac{2\pi\nu d}{c(1-R)}; \quad (15)$$

and the finesse by

$$F = \frac{\pi}{l(1-R)}. \quad (16)$$

We thus see that the instrumental bandwidth and  $Q$  of a mode-degenerate interferometer are the same as for a general spherical-mirror interferometer or a Fabry-Perot etalon, but that the free-spectral-range, finesse, and peak transmission are reduced by a factor  $l$ . We can also see why the confocal interferometer is the most useful mode-degenerate interferometer: it has the highest finesse of any mode-degenerate interferometer. (The concentric interferometer, which corresponds to  $l = 1$ , is not mode-degenerate; the theory leading to equation (8) is not valid in the concentric limit.)

Mode-degenerate interferometers can also be analyzed in terms of geometrical optics<sup>4</sup>. The condition expressed in equation (9) is equivalent to the condition that a ray launched in the cavity retrace its path after  $l$  complete traversals of the cavity. Thus, from the standpoint of geometrical optics, an  $l$ -fold mode-degenerate interferometer appears to have an effective length which is  $l$  times the actual distance between the mirrors. A typical ray path for a confocal interferometer is shown in Figure 2.



2. Ray paths in a confocal interferometer.

The factors which limit the performance of mode-degenerate interferometers are the reflectance of the mirrors, the surface figure of the mirrors, and the spherical aberration of the mirrors.

The limitation imposed by the reflectance of the mirrors is not usually serious. It is now possible to obtain mirrors having a reflectance of greater than .998. In a confocal interferometer, this corresponds to a finesse (c.f. equation 16) of more than 750. Such values of finesse have been realized experimentally.

The surface figure requirement on the interferometer mirrors presents a somewhat more serious problem. As is the case for a Fabry-Perot etalon, the surface figure must be accurate to roughly the transmission wavelength divided by the finesse. In order to minimize the requirements on the surface

figure of the mirrors, the diameter of the incoming laser beam should be approximately equal to the diameter of the  $TEM_{00}$  mode of the interferometer.

Spherical aberration of the mirrors gives rise to a fundamental limitation on the amount of mode-mismatch that can be tolerated in a mode-degenerate interferometer. The theory of Hermite-Gaussian mode structure in spherical-mirror interferometers is based on the paraxial-optics approximation. If a mode-degenerate interferometer is illuminated too far off-axis, the paraxial-optics approximation cannot be used to describe its behavior. The dominant aberration which enters the theory is spherical aberration. The amount of spherical aberration in the interferometer depends on the radius of curvature and separation of the mirrors.

For a confocal interferometer, one can show that the path-difference variation, caused by spherical aberration, for rays entering the interferometer parallel to the axis, but displaced from it by a distance  $h$ , is given by

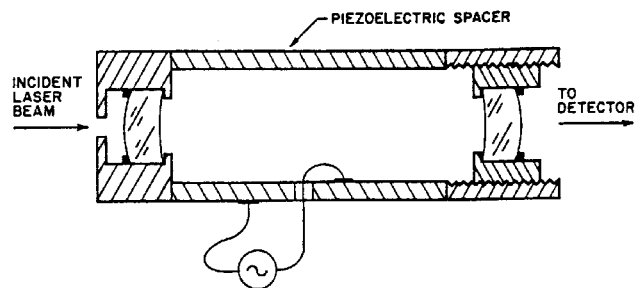
$$\Delta = -\frac{h^4}{d^3}. \quad (17)$$

If we demand that this path-difference variation be less than the transmission wavelength of the interferometer divided by the finesse, we find that the incoming beam must have a radius  $h$  given by

$$h < \left(\frac{\lambda d^3}{F}\right)^{1/4}. \quad (18)$$

## V. Experimental Properties of Mode-Degenerate Interferometers

In this section, we consider some of the practical aspects of mode-degenerate interferometers. As discussed in the preceding section, the confocal interferometer is the most useful of the mode-degenerate interferometers, because it has the highest finesse. Most of the discussion in this section is specifically, but not inevitably, related to the confocal interferometer.



3. Scanning confocal interferometer.

Figure 3 shows a typical scanning confocal interferometer. It comprises two spherical mirrors, separated by a distance equal to their radius of curvature. The back surfaces of the mirrors are made such that the mirrors are self-collimating: that is, a plane wavefront incident on the interferometer will be transformed into a spherical wavefront whose radius of curvature matches that of the transverse modes of the interferometer. The concave surfaces of the mirrors are coated with high-reflectance multilayer films, and the convex surfaces are coated with anti-reflection films to eliminate spurious interferometer resonances involving the back surfaces of the mirrors.

The mirrors are mounted in cells which are separated by a piezoelectric spacer. By applying a potential difference of a few hundred volts to the piezoelectric spacer, the separation of the mirrors can be varied by a few wavelengths. In practice, a sawtooth or sinusoidal waveform is usually applied to the piezoelectric spacer to scan the separation of the interferometer mirrors. For a confocal interferometer, a change in separation of the mirrors of one-fourth wavelength scans the interferometer through one free-spectral-range.

An aperture is placed outside the entrance mirror to limit the diameter of the incident beam. The upper limit on the aperture size can be determined using equation (18). If the beam entering the interferometer is collimated, no further apertures are required. However, if the interferometer is used with non-collimated beams, it is also necessary to use an aperture on the exit of the interferometer to eliminate the reduction in finesse caused by spherical aberration in the mirrors. The use of this second aperture will reduce the peak transmission of the interferometer, and it is generally more desirable to focus the incoming beam properly, rather than use a second aperture.

The light transmitted by the interferometer is detected by a photocell or photomultiplier, and the output signal of the photodetector is recorded on an oscilloscope, as a function of the voltage applied to the piezoelectric spacer. The oscilloscope thus displays a signal which is equivalent to the laser mode intensity vs. optical frequency.

It is important that the mirror separation be quite close to confocal. The tolerance on the mirror spacing depends on the length of the interferometer and its finesse. For very short, high-finesse interferometers, the mirror spacing should be set to within a few wavelengths. In practice, the adjustment of length is quite easy to make. The mirror spacing should be set so that it is approximately confocal. By observing the mode structure of a laser on an oscilloscope, the final adjustment of the mirror spacing can then be made to maximize the

finesse of the interferometer. Once the separation of the interferometer mirrors is set, it needs no further adjustment.

The actual use of confocal interferometers is quite simple: basically, they need only be placed in a laser beam and adjusted so that the beam is reflected more or less back on itself. With a relatively crude alignment, fringes will be obtained. To achieve the maximum finesse, the angle should be adjusted fairly carefully to ensure that the interferometer axis is close to the axis of the incident beam. To perform the fine-angle adjustment, it is convenient to mount the interferometer on an adjustable-angle mirror mount.

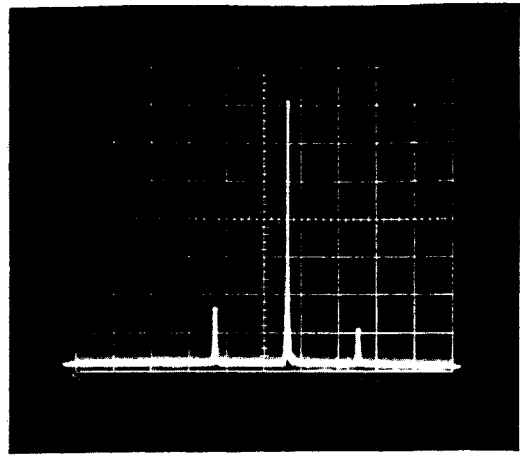
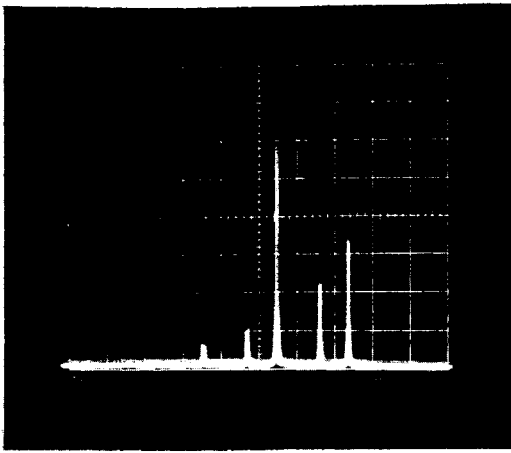
It is usually desirable to put an optical isolator, such as a circular polarizer, in the beam between the laser and the interferometer, even when the interferometer is illuminated off-axis. The reason for this is that there is usually a certain amount of back-scatter from the interferometer mirrors. Although the specular reflection from the interferometer mirrors does not retro-reflect into the laser, the back-scatter can, in some cases, perturb the modes of the laser.

## VI. Applications of Scanning Spherical-Mirror Interferometers

As stated in the introduction, scanning spherical-mirror interferometers are useful for studying the general mode structure of gas lasers. In this section, we consider two specific applications.

The first application of scanning spherical-mirror interferometers that we consider is their use in adjusting a laser so that it operates in a single transverse mode. The conventional method for making such an adjustment consists of visually observing the intensity distribution in the output beam of the laser while adjusting the mirrors. When the output beam has an apparently Gaussian intensity distribution, the laser is assumed to be oscillating in the  $TEM_{00}$  transverse mode.

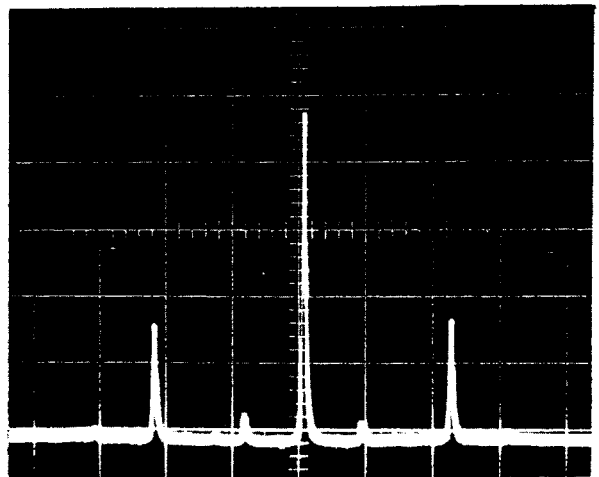
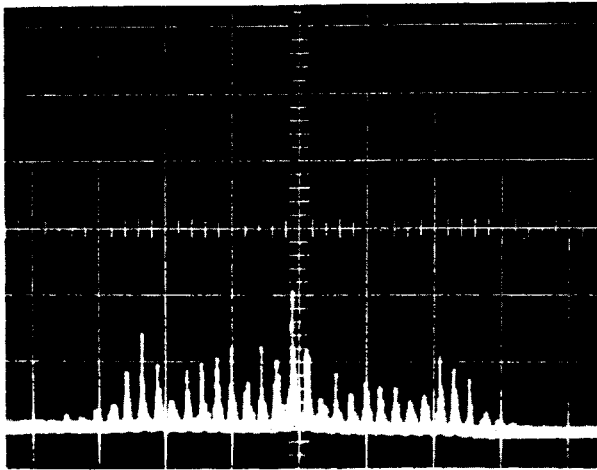
The above method for adjusting a laser is somewhat unreliable; often lasers which appear to be operating in a single transverse mode actually are oscillating simultaneously in two transverse modes. This double oscillation can be detected easily using a scanning (mode-degenerate) spherical-mirror interferometer. Figure 4 shows the mode spectra obtained when a typical helium-neon laser is operating in (a) two transverse modes, and (b) a single transverse mode.



4. (a) Output spectrum of a helium-neon laser operating simultaneously in two transverse modes.

(b) Output spectrum of a helium-neon laser operating in a single transverse mode.

The vertical sensitivity and horizontal dispersion are the same for both (a) and (b).



5. (a) Output spectrum from a free-running argon ion laser.

(b) Output spectrum from a self-phase-locked argon ion laser.

The vertical sensitivity and horizontal dispersion are the same for both (a) and (b).

The other application of scanning spherical-mirror interferometers that we consider is their use in studying phase-locking phenomena. Figure 5 shows the output spectrum of a single transverse-mode argon-ion laser when it is (a) free running, and (b) self phase-locked. Note that the output spectrum is quite different for the two cases. The spectrum shown in Figure 6(a) is somewhat

blurred because of the erratic mode-hopping during the exposure time. This mode-hopping is characteristic of lasers whose mode spacing is less than the homogeneous linewidth. In Figure 6(b), the output spectrum is constant in time.

Douglas C. Sinclair  
April, 1968

## References

1. R. L. Fork, D. R. Herriott, and H. Kogelnik, "A Scanning Spherical Mirror Interferometer for Spectral Analysis of Laser Radiation," *Appl. Optics* **3**, 1471 (1964).
  2. P. Connes, "Increase of the Product of Luminosity and Resolving Power of Interferometers by Using a Path Difference Independent of the Angle of Incidence," *Revue d'Optique* **35**, 37 (1956).
  3. A. L. Bloom, "Properties of Laser Resonators Giving Uniphase Wave Fronts," *Spectra-Physics Laser Technical Bulletin No. 2*, Mountain View, California (1963).
  4. D. R. Herriott, H. Kogelnik, and R. Kompfner, "Off-Axis Paths in Spherical-Mirror Interferometers," *Appl. Optics* **3**, 523 (1964).
-